

# Reprogramming EF-hands for design of catalytically amplified lanthanide sensors

Korrie L. Mack · Olesia V. Moroz ·  
Yurii S. Moroz · Alissa B. Olsen ·  
Jaclyn M. McLaughlin · Ivan V. Korendovych

Received: 1 December 2012 / Accepted: 30 January 2013 / Published online: 19 February 2013  
© SBIC 2013

**Abstract** We recently reported that a computationally designed catalyst nicknamed AlleyCat facilitates C–H proton abstraction in Kemp elimination at neutral pH in a selective and calcium-dependent fashion by a factor of approximately 100,000 (Korendovych et al. in *Proc. Natl. Acad. Sci. USA* 108:6823, 2011). Kemp elimination produced a colored product that can be easily read out, thus making AlleyCat a catalytically amplified metal sensor for calcium. Here we report that metal-binding EF-hand motifs in AlleyCat could be redesigned to incorporate trivalent metal ions without significant loss of catalytic activity. Mutation of a single neutral residue at position 9 of each of the EF-hands to glutamate results in almost a two orders of magnitude improvement of selectivity for trivalent metal ions over calcium. Development of this new lanthanide-dependent switchable Kemp eliminase, named CuSeCat EE, provides the foundation for further selectivity improvement and broadening the scope of the repertoire of metals for sensing. A concerted effort in the design of switchable enzymes has many environmental, sensing, and metal ion tracking applications.

**Keywords** Protein design · Metal sensor · Lanthanides

## Introduction

Metal sensing is important in a variety of applications ranging from metal tracking in living cells to detection of toxic metal ions in the environment. Considerable effort has been dedicated to the development of small-molecule metal sensors; however, such sensors are often expensive, difficult to design, and not always compatible with living organisms [1]. On the other hand, protein-based sensors are inherently biocompatible and biodegradable and can be potentially expressed as a fusion tag, offering new opportunities to track metals in vivo. Available protein-based sensors are based on inhibitory properties of metal ions [2], fluorescence of green fluorescent protein [3], or fluorescence resonance energy transfer [4, 5]. These systems are either very bulky or suffer from low sensitivity and selectivity. The concept of catalytically amplified sensing, where an allosteric binding event is linked to catalysis, has emerged as a powerful tool to overcome these limitations [6, 7]. The few reported examples of this method [6, 8] are not easily generalizable and rely mostly on small-molecule ligands for metal binding. Our research efforts are directed toward the design of a new enzymatic platform, which will link metal binding to de novo designed catalytic sites. This is achieved by connecting a metal-binding protein domain through a linker to a catalytic domain, performing an unnatural reaction to produce a colored or fluorescent product (Fig. 1). Binding of a metal ion will result in a conformational change propagated through a linker domain to the catalytic domain, which in turn will assume a catalytically competent conformation. The key advantages of this approach are (a) directed evolution can be applied to these sensors to improve selectivity and specificity for metal ion binding, (b) the metal-binding domain and the catalytic domain

**Electronic supplementary material** The online version of this article (doi:10.1007/s00775-013-0985-5) contains supplementary material, which is available to authorized users.

K. L. Mack · O. V. Moroz · Y. S. Moroz ·  
A. B. Olsen · J. M. McLaughlin · I. V. Korendovych (✉)  
Department of Chemistry, Syracuse University,  
Syracuse, NY 13244, USA  
e-mail: ikorendo@syr.edu

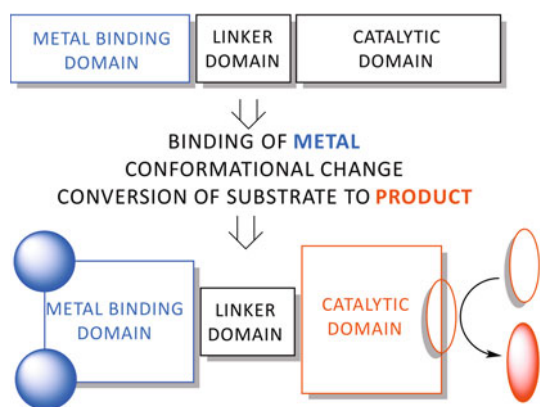
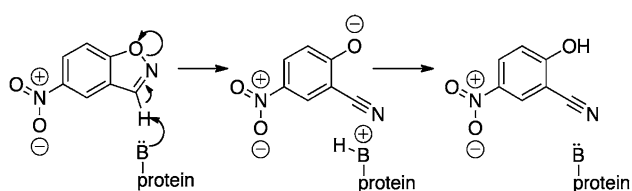


**Fig. 1** The general principle of metal sensing by CuSeCat



**Scheme 1** Kemp elimination reaction

can be developed (and used!) independently, (c) the protein sensor can be easily obtained recombinantly, and (d) these sensors can be expressed as fusion tags to proteins and thus may provide detailed information about local metal concentrations in vivo.

Previously we have shown that this goal can be accomplished using a simple protein scaffold containing an EF-motif and a de novo designed active site [9]. A single mutation conferred the ability to catalyze an unnatural reaction, Kemp elimination (Scheme 1), on a nonenzymatic scaffold. Importantly, Kemp elimination proceeded only in the presence of Ca<sup>2+</sup>, which led to a conformational change to allow catalysis. The resulting catalyst, named AlleyCat, is thus a catalytically amplified sensor for calcium. Kemp elimination provides an excellent readout as the substrate is easily available, the product can be easily measured spectrophotometrically, and there are no natural proteins in *Escherichia coli* that perform this reaction. The formation of the yellow product can be easily monitored even in crude cell lysates. But is AlleyCat just a single lucky example of protein design? Could it be adjusted to sense other metals and could the catalytic and the sensing domains be tuned separately?

In this paper we show that the two domains are effectively separated in AlleyCat and could be evolved to sense metals other than calcium. These results pave way to further improvement and diversification of catalytically amplified sensors that combine the power of protein design with diversity of metal-binding domains.

## Materials and methods

### General

Reagents and buffers were purchased from BioBasic and Santa Cruz Biotechnology. All measurements were done in deionized Milli-Q water. DNA oligonucleotides were purchased from Integrated DNA Technologies. Enzymes for cloning were purchased from Promega. TEV protease was expressed and purified according to the literature procedure [10].

### Cloning and mutagenesis

All the genes described in this article were cloned into pEXP5-NT expression vector (Invitrogen), which contains an N-terminal His<sub>6</sub>-tag separated from the gene of interest by a TEV protease recognition fragment (GENLYFQSL). The appropriate mutations were introduced using a standard mutagenesis protocol that uses *PfuTurbo* DNA polymerase provided by the manufacturer. After the PCR step, the template was digested with *DpnI* restriction enzyme and transformed into *E. coli* XL-10 cells. DNA from several colonies was extracted, and sequences of the mutated genes were confirmed by Sanger sequencing (Genewiz). The plasmids of the designed catalysts were deposited in AddGene.

### Protein expression and purification

The pEXP5-NT vectors containing the genes of interest were transformed into *E. coli* BL21(DE3) pLysS cells and expressed using ZYM-5052 autoinduction medium [11]. The cells were then collected by centrifugation and lysed by sonication in lysis buffer containing 25 mM *N*-(2-hydroxyethyl)piperazine-*N'*-ethanesulfonic acid (HEPES), 20 mM imidazole, 10 mM CaCl<sub>2</sub>, and 300 mM NaCl (pH 8) on ice with protease inhibitor (phenylmethylsulfonyl fluoride) added. The crude cell lysate was then centrifuged at 17,000g for 1 h, and the supernatant was applied onto a nickel nitrilotriacetic acid column. After several rounds of washing, the protein was eluted with buffer containing 25 mM HEPES, 500 mM imidazole, 10 mM CaCl<sub>2</sub>, and 300 mM NaCl (pH 8). Up to 15 mM EDTA was added to the purified sample, and the buffer was exchanged twice to 20 mM 2-(*N*-morpholino)ethanesulfonic acid (MES), 100 mM NaCl (pH 6) by applying the sample onto a Bio-Rad 10 DG desalting column to remove metal ions and EDTA. The purity of the proteins was established by sodium dodecyl sulfate polyacrylamide gel electrophoresis (Figs. S1, S2).

### Kinetic assays

Kinetic measurements were done with a Thermo Labsystems Multiskan Spectrum plate reader monitoring

absorbance at 380 nm at 22 °C using at least three independent measurements as previously described [9, 12]. EDTA (15 mM) was added to the protein stocks to exclude any adventitious metal binding, and the resulting apoprotein was recovered by buffer exchange on a desalting column. Unless specifically stated, the final protein concentration (determined by UV–vis spectroscopy using  $\epsilon_{280} = 4,450 \text{ M}^{-1} \text{ cm}^{-1}$ ) [13] for kinetic measurements was 2  $\mu\text{M}$ . Enzyme activity in the presence of saturating concentration of  $\text{CaCl}_2$  (10 mM) was characterized in a buffer containing 10 mM 2-morpholinoethanesulfonic acid (MES) at pH 6 and 100 mM NaCl, with the substrate concentrations ranging from 0.1 to 1 mM. Kinetic parameters ( $k_{\text{cat}}$  and  $K_{\text{M}}$ ) were obtained by fitting the data to the Michaelis–Menten equation:  $\{v_0 = k_{\text{cat}}[\text{E}]_0[\text{S}]_0 / (K_{\text{M}} + [\text{S}]_0)\}$ .  $k_{\text{cat}}/K_{\text{M}}$  values were obtained by fitting the linear portion of the plot to  $v_0 = (k_{\text{cat}}/K_{\text{M}})[\text{E}]_0[\text{S}]_0$ . For pH profile studies, the following buffers were used at a final concentration of 25 mM: citrate (pH 4.5–5.5), MES (pH 6–6.5), HEPES (pH 7–8), tris(hydroxymethyl)aminomethane (pH 8.5). The maximum  $k_{\text{cat}}/K_{\text{M}}$  values were obtained from fitting the pH dependence data to  $k_{\text{cat}}/K_{\text{M}} = (k_{\text{cat}}/K_{\text{M}})_{\text{protonated}} + (k_{\text{cat}}/K_{\text{M}})_{\text{deprotonated}} \times 10^{-\text{p}K_{\text{a}}} / (10^{-\text{pH}} + 10^{-\text{p}K_{\text{a}}})$ , where  $\text{p}K_{\text{a}}$  is the apparent  $\text{p}K_{\text{a}}$  of the active residue. The dependence of protein activity as a function of added metal concentration was done in buffer containing 20 mM MES and 100 mM NaCl at pH 6 at a 500  $\mu\text{M}$  substrate concentration. In conditions with zero concentration of metal, 5  $\mu\text{M}$  EDTA was included to exclude any possibility of adventitious metal binding. Metal dependence profiles were determined at the following metal concentrations: 0–10 mM  $\text{CaCl}_2$  for CuSeCat and CuSeCat EE, and 0–0.1 mM and 0–32  $\mu\text{M}$  trivalent metals for CuSeCat EE and CuSeCat, respectively. The data were fit to the Hill equation [14]:

$$\frac{k_{\text{cat}}/K_{\text{M}}}{(k_{\text{cat}}/K_{\text{M}})_{\text{Max}}} = \frac{\left(\frac{[\text{M}]_{\text{tot}}}{M_{50}}\right)^h}{1 + \left(\frac{[\text{M}]_{\text{tot}}}{M_{50}}\right)^h} \quad (1)$$

where  $k_{\text{cat}}/K_{\text{M}}$  is enzymatic efficiency at the total metal concentration of  $[\text{M}]_{\text{tot}}$ ,  $h$  is the Hill coefficient,  $M_{50}$  is the metal concentration that induces 50 % enzymatic activity, and  $(k_{\text{cat}}/K_{\text{M}})_{\text{max}}$  is the maximum enzymatic efficiency.

### Circular dichroism spectroscopy

The circular dichroism (CD) spectra were collected with a JASCO J-715 CD spectrometer using a step scan mode (4-s averaging time for every point) averaging over three runs using a quartz cuvette with a 1-mm path length. The protein concentration was held at 25  $\mu\text{M}$ . The typical buffer conditions were 4 mM MES (pH 6) and 30 mM NaCl at different concentrations of metal ions. Care was taken so

the sample absorbance never exceeded 1.5 at all wavelengths to produce reliable mean residue ellipticity values. The chemical denaturation experiments were conducted by monitoring ellipticity of proteins at 222 nm in the presence of various concentrations of guanidinium chloride (0–6 M). The protein concentration was held at 25  $\mu\text{M}$ . The typical buffer conditions were 4 mM MES (pH 6), 2 mM  $\text{CaCl}_2$ , and 30 mM NaCl. The chemical denaturation data were fit to the following expression:

$$MRE = \frac{MRE_f + MRE_{u1} e^{-\frac{\Delta G_1 - m_1 [D]}{RT}}}{1 + MRE_{u1} e^{-\frac{\Delta G_1 - m_1 [D]}{RT}}} + \frac{MRE_{f1} + MRE_u e^{-\frac{\Delta G_2 - m_2 [D]}{RT}}}{1 + MRE_u e^{-\frac{\Delta G_2 - m_2 [D]}{RT}}}$$

where MRE is the observed mean residue ellipticity,  $MRE_f$  and  $MRE_{u1}$  are mean residue ellipticities representing the folded and unfolded states of the C-terminal domain, respectively,  $MRE_{f1}$  and  $MRE_u$  are mean residue ellipticities representing the folded and unfolded states of the N-terminal domain, respectively,  $[D]$  is the concentration of denaturant, and  $\Delta G_1$  and  $\Delta G_2$  are free energies of unfolding of the C-terminal domain and the N-terminal domain, respectively [15].

### NMR studies

Proteins for NMR studies were expressed on an M9 minimal medium containing  $^{15}\text{N}$ -labeled  $\text{NH}_4\text{Cl}$  using established protocols [16]. The 2D  $^1\text{H}$ – $^{15}\text{N}$  heteronuclear single quantum coherence (HSQC) spectra were acquired in a buffer containing 10 mM  $\text{CaCl}_2$ , 20 mM HEPES (pH 6.9), 100 mM NaCl at 30 °C and 10 %  $\text{D}_2\text{O}$  with a Bruker AVANCE III NMR spectrometer operating at 600 MHz. The water signal was suppressed using presaturation. The chemical shifts were referenced by 2,2-dimethylsila-pentane-5-sulfonic acid added as an internal standard.

## Results and discussion

### Protein design

The basic principle behind the design of AlleyCat is the ability of a metal-binding motif (EF-hand) in calmodulin to stabilize a protein fold, where a large portion of the hydrophobic region of the protein is exposed to solvent. We took advantage of the energy provided by metal binding to introduce a charged residue, glutamate, in a hydrophobic pocket of the protein in a conformation suitable for performing Kemp elimination. By the virtue of the glutamate residue being in the hydrophobic environment, the  $\text{p}K_{\text{a}}$  of the glutamate side chain increased, giving an

overall five orders of magnitude improvement in the rate of the catalyzed reaction compared with the noncatalyzed reaction. Inspection of AlleyCat's structure (Fig. 2) shows that this protein catalyst can potentially fulfill the requirements set in "Introduction" to create a catalytically amplified sensor for metal ions. The metal-binding loops, shown in blue in Fig. 2, are separate from the catalytic region, shown in green, and the catalytic E92 residue (red) pointing in the middle of the hydrophobic pocket of the protein. The idea behind the design is simple: we need to alter the specificity of the metal-binding loops so the catalyst can bind other metals while retaining its catalytic properties. EF-hand is one of the most studied metal-binding protein motifs. It binds calcium ions tightly and selectively [17] and can be redesigned to selectively bind a variety of other metals [18–21]. Importantly, binding of metals to EF-hand induces a large conformational change in neighboring regions.

Our design started with one of the improved versions of AlleyCat taken from the library of variants identified through several rounds of directed evolution by saturation mutagenesis in the positions immediately facing the substrate binding pocket followed by error-prone PCR [22]. Unlike AlleyCat, the proteins in this library have both N-terminal and C-terminal domains that lower the toxicity in *E. coli* and provide an additional handle for purification. The mutant chosen has five extra mutations relative to the original sequence of chicken calmodulin in addition to the F92E active base: V91M, H107I, L112R, M144R, and T146R (the full sequence is presented in Table S1). We have named the mutant Customizable Sensor aided by Catalysis (CuSeCat). CuSeCat was prepared by overexpression in *E. coli* using autoinduction medium as described in detail in "Materials and methods."

## Kinetic characterization of CuSeCat

Having modified the catalytic domain of the protein, we needed to characterize the activity of CuSeCat for Kemp elimination and to determine whether its activity is still strictly calcium dependent. The pH profile of the activity shows that the maximum  $k_{\text{cat}}/K_{\text{M}}$  for CuSeCat reaches  $253 \pm 4 \text{ M}^{-1} \text{ s}^{-1}$ , which is about 50 times higher than the corresponding  $k_{\text{cat}}/K_{\text{M}}$  for AlleyCat (Table 1). The individual  $k_{\text{cat}}$  and  $K_{\text{M}}$  values, determined from Michaelis–Menten plots, are given in Table 1. The representative plots and the corresponding fits are presented in Figs. S3 and S4. Mutation of the active residue (E92Q) leads to a complete loss of activity, confirming that the introduction of additional mutations did not change the catalytic mechanism. Removal of the His<sub>6</sub> affinity tag had little effect on the overall protein activity. Importantly, CuSeCat possesses the same calcium dependence as AlleyCat (Fig. 4), which allowed us to proceed to the next step—reprogramming the catalyst to sense other metals.

## Redesigning the metal-binding site

Although the EF-hand binding motif is specific for calcium, it is known to bind other metals. Drake et al. [23–25] investigated the factors that influence the selectivity of the metal-binding domains and showed that both metal size and metal charge are effective determinants of EF-hands. In particular, they found that residue 9 of the 12-residue EF-hand loop influences its affinity for calcium the most. Mutation of neutral residues at position 9, called a gateway position, to negatively charged glutamate/aspartate increased the overall charge of the EF-hand and thus increased its affinity for  $\text{M}^{3+}$  ions. Effectively, the gateway

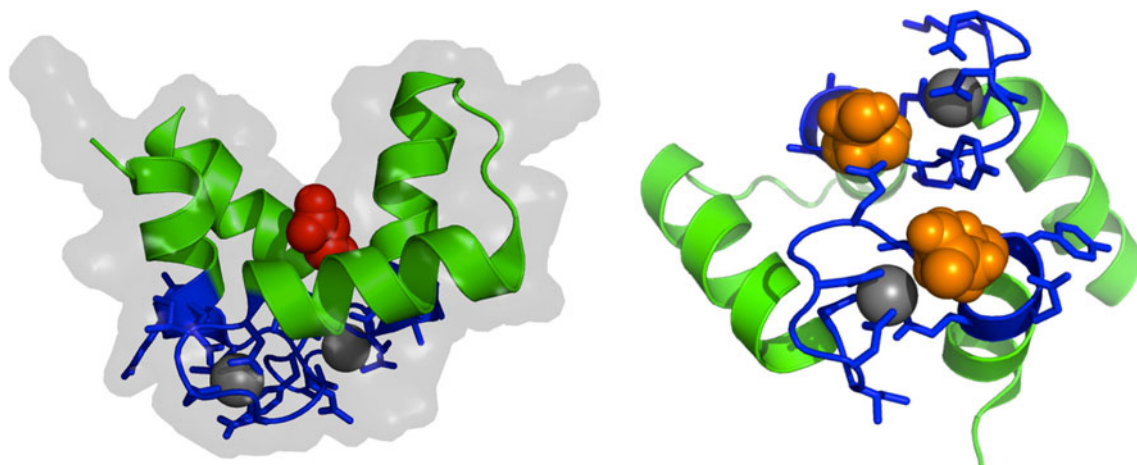


**Fig. 2** *Left:* The structure of AlleyCat (based on Protein Data Bank entry 2KZ2) showing the EF-hand metal-binding domain in *blue*, the catalytic domain in *green*, and the catalytic E92 residue in *red*. *Right:*

The view of the metal-binding loops in AlleyCat. The residues responsible for selectivity of EF-hands for divalent metal ions (S101 and N137) are shown in *orange*

**Table 1** Kinetic parameters for the prepared proteins ( $k_{\text{cat}}$ ,  $K_{\text{M}}$ , and  $k_{\text{cat}}/K_{\text{M}}$  values are reported at pH 6) in the calcium-saturated state

Protein	$k_{\text{cat}}$ ( $\text{s}^{-1}$ )	$K_{\text{M}}$ (mM)	$k_{\text{cat}}/K_{\text{M}}$ ( $\text{s}^{-1} \text{M}^{-1}$ )	$(k_{\text{cat}}/K_{\text{M}})_{\text{max}}$ ( $\text{s}^{-1} \text{M}^{-1}$ )	$\text{p}K_{\text{a}}$
CuSeCat	$0.16 \pm 0.02$	$4.1 \pm 0.8$	$37 \pm 2$	$253 \pm 4$	$6.75 \pm 0.02$
CuSeCat DD	$0.18 \pm 0.04$	$4.6 \pm 1.3$	$38 \pm 1$	$281 \pm 4$	$6.73 \pm 0.02$
CuSeCat EE	$0.08 \pm 0.01$	$2.5 \pm 0.3$	$29 \pm 1$	$143 \pm 3$	$6.61 \pm 0.03$
CuSeCat D131N	$0.21 \pm 0.03$	$5.3 \pm 0.8$	$37 \pm 2$	$274 \pm 4$	$6.73 \pm 0.03$
CuSeCat D133N	$0.28 \pm 0.06$	$6.1 \pm 1.3$	$43 \pm 1$	$372 \pm 4$	$6.64 \pm 0.02$
CuSeCat no tag	$0.24 \pm 0.04$	$4.9 \pm 0.9$	$46 \pm 2$		
CuSeCat DD no tag	$0.25 \pm 0.04$	$5.8 \pm 1.0$	$41 \pm 2$		
CuSeCat E92Q	ND	ND	$0.09 \pm 0.01$		
CuSeCat DD E92Q	ND	ND	$0.09 \pm 0.01$		

ND not determined

position serves as a charge-based selectivity filter for metal ions. On the basis of these findings we decided to explore the role of the selectivity filter residues in a de novo designed protein. The role of the selectivity filter has been well established in an isolated metal-binding loop in a galactose-binding protein, but would the same still hold true for a de novo designed catalytic protein that has a pair of EF-hands closely associated with each other? To test this hypothesis we mutated the position 9 residues in the C-terminal EF-hand domains that are responsible for CuSeCat's selectivity for calcium. The neutral residues S101 and N137 (Fig. 2) were both mutated to aspartates and glutamates to produce proteins named CuSeCat DD (CuSeCat with S101D and N137D mutations) and CuSeCat EE (CuSeCat with S101E and N137E mutations). Additionally, we decided to explore the role of conservative aspartate to asparagine mutations in EF-hands to determine whether lowering the charge will lead to relative improvement of the protein's affinity for calcium over  $\text{M}^{3+}$  metals. These mutations were introduced at positions 3 and 5 of the EF-hand, giving the corresponding mutants CuSeCat D131N and CuSeCat D133N. All the mutants were expressed and purified and were shown to be stable and folded (vide infra).

#### CD and NMR studies

The CD signature of calmodulin is very characteristic in the apo and the holo forms and allows quick determination of the overall fold. The CD spectra of the designed proteins were collected in the absence of metal, in the presence of 2 equiv of  $\text{Ca}^{2+}$  and  $\text{Tb}^{3+}$ , and in the presence of 80 equiv of  $\text{Ca}^{2+}$ . The C-terminal domain is known to bind calcium cooperatively with higher overall affinity compared with the N-terminal domain [26]. The spectrum with 2 equiv of metal ions should represent the metal-saturated C-terminal domain; the spectra with 80 equiv of  $\text{Ca}^{2+}$  provide the signature of the holo form. The results of the CD

experiments are presented in Fig. 3. The original catalyst, CuSeCat, and both mutants (CuSeCat DD and CuSeCat EE) show a distinct helical signature, characteristic of the apocalmodulin fold. The helicity slightly decreases upon introducing additional carboxylates into EF-hands, with glutamate being more destabilizing than aspartate. The CD spectra of the mutants upon addition of metal ions show distinctly different behavior. The CD spectrum of CuSeCat does not change upon addition of 2 equiv of  $\text{Tb}^{3+}$ , but addition of  $\text{Ca}^{2+}$  results in increased helicity characteristic of holocalmodulin. The change is dependent on the concentration of the added metal: the increase for the saturating amount (80 equiv) is roughly double that for 2 equiv of  $\text{Ca}^{2+}$ . This is consistent with the overall 1:4 stoichiometry of metal binding (CuSeCat has a total of four EF-hands) and similar secondary structure of the two domains of calmodulin. The behavior of CuSeCat EE is switched: the saturating amount of calcium brings the helicity up to the values of holo-CuSeCat, but the addition of 2 equiv of  $\text{CaCl}_2$  has little effect on the CD spectrum. On the other hand, addition of just 2 equiv of  $\text{TbCl}_3$  results in a spectrum essentially identical to that of the calcium-saturated holo-CuSeCat. In the case of CuSeCat DD, both  $\text{Ca}^{2+}$  and  $\text{Tb}^{3+}$  exert similar effects on the CD spectra. These results suggest that the specificity of CuSeCat DD and CuSeCat EE is switched to favor the trivalent metal ion, and CuSeCat EE shows higher affinity for terbium, consistent with the findings of Falke et al.

Although CD spectra provide a picture of the overall secondary structure, they do not necessarily prove that the overall protein fold remains intact in the designed mutants. We used NMR spectroscopy to investigate the differences between the structures of CuSeCat DD, CuSeCat EE, and calmodulin in the metal-bound states. Previously, we showed that introduction of the F92E mutation into the calmodulin scaffold does not change the fold of the C-terminal domain of calmodulin (root mean square deviation of approximately 1.35 Å) [9]. Earlier NMR studies of

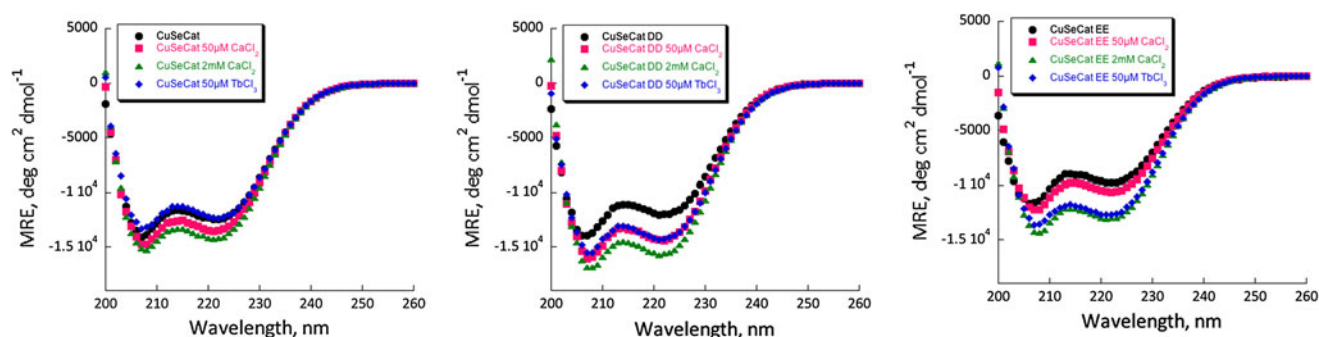


**Fig. 3** Circular dichroism spectra of CuSeCat (*left*), CuSeCat DD (*center*), and CuSeCat EE (*right*) in the absence of metals (*black*), in the presence of 2 equiv of  $\text{CaCl}_2$  (*red*), in the presence of 80 equiv of

$\text{CaCl}_2$  (*green*), and in the presence of 2 equiv of  $\text{TbCl}_3$  (*blue*). MRE is mean residue ellipticity

calmodulin showed that the C-terminal and N-terminal domains of the protein are essentially independent of each other in the absence of the natural binding partner [27]. We acquired an  $^1\text{H}$ – $^{15}\text{N}$ , HSQC spectrum of a uniformly  $^{15}\text{N}$  labeled full-length calmodulin F92E mutant (Fig. S5). The positions of the peaks are consistent with the previously published NMR structures of the full wild-type N-terminal domain and the C-terminal domain with an F92E mutation. The HSQC spectra of CuSeCat DD, CuSeCat EE, and CuSeCat, overlaid in Fig. S6, indicate high structural similarity for the three mutants and are characteristic of the calmodulin fold (as shown by the overlay of the spectra of CuSeCat and calmodulin F92E).

#### Kinetic characterization of the CuSeCat mutants

The structural data described so far establish similarities between CuSeCat and its mutants, but are the S101D/E and N137D/E mutations sufficiently conservative to preserve catalytic activity in the Kemp elimination reaction? The  $k_{\text{cat}}/K_M$ ,  $(k_{\text{cat}}/K_M)_{\text{max}}$ , and  $\text{p}K_a$  values for CuSeCat DD are essentially identical to those for CuSeCat, indicative of minimal disruption of the catalytic domain. Replacing the catalytic Glu92 residue with glutamine completely eliminates the activity, confirming that the newly introduced mutations have not influenced the mechanism of catalysis. The S101E and N137E mutations proved to be more disruptive: the catalytic efficiency of CuSeCat EE is about twofold lower and the  $\text{p}K_a$  of the active base decreased as well (Table 1). Interestingly, the mutations designed to lower the overall charge of the metal-binding domain (D131N and D133N) did not result in any activity loss, and in one case (D133N) even produced an approximately 50 % increase in catalytic efficiency. Interestingly, the mutants with the highest activity changes (CuSeCat EE and CuSeCat D133N) show substantially lower affinity for  $\text{Ca}^{2+}$  (vide infra) and smaller unfolding energies, as demonstrated by chemical denaturation studies (Fig. S7, Table S2).

Next, we explored the dependence of activity as a function of added metal ion concentration. We compared the activity of CuSeCat and its mutants for  $\text{Ca}^{2+}$  with that of  $\text{Y}^{3+}$  (a trivalent  $4d$  metal), and the lanthanides  $\text{Pr}^{3+}$ ,  $\text{Nd}^{3+}$ ,  $\text{Sm}^{3+}$ ,  $\text{Tb}^{3+}$ , and  $\text{Yb}^{3+}$ , which represent a wide range of ionic radii (the effective ionic radius for a coordination number of seven is 1.06 Å for  $\text{Pr}^{3+}$  and 0.92 Å for  $\text{Yb}^{3+}$ ) and at the same time allow the activity of ions of very similar sizes (1.06 Å for  $\text{Pr}^{3+}$ , 1.05 Å for  $\text{Nd}^{3+}$ , and 1.02 Å for  $\text{Sm}^{3+}$ ) to be compared. Binding of metal ions to calmodulin is known to be cooperative, and the two domains have different binding constants [26, 28]. Determination of the true binding constants for every EF-hand of each protein is a complex task. For the purpose of this work we are only interested in the response of the Kemp elimination activity of the catalyst as a function of metal ion. The response curve is well described by an empirical Hill model. By comparing the  $M_{50}$  values (concentration of metal that provides 50 % catalytic activity at a constant protein concentration) obtained from the fits, we can quantitatively describe the relative specificity of the designed mutant for different ions. The kinetic studies were performed at pH 6 to ensure that the metal ions were in the  $\text{M}^{3+}$  state and to minimize hydrolytic effects.

A summary of the activity of the designed mutants in the presence of different metals is given in Table 2 and Fig. 4; the raw data and the corresponding fits are provided in Figs. S8–S10. Although the maximum catalytic efficiencies of CuSeCat, CuSeCat DD, CuSeCat D131N, and CuSeCat D133N are similar, their calcium dependence varies drastically. Introducing two aspartate residues at the 9 positions of EF-hands has only a mild effect on the protein's affinity for calcium, whereas single mutations at positions 3 (D131N) and, especially, 5 (D133N) affect the corresponding  $M_{50}$  values by eightfold and 26-fold, respectively. Interestingly, CuSeCat D131N, which has the lowest affinity for  $\text{Ca}^{2+}$ , displays the highest enzymatic efficiency. Similarly to D131N, glutamate residues at

position 9 strongly affect the affinity for calcium:  $M_{50}$  for CuSeCat EE is 25-fold higher than that for CuSeCat. CuSeCat's lanthanide affinity is similar to its calcium affinity (Table 2), with no clear trend based on the ionic radius of the trivalent metal. Despite a substantial decrease of  $M_{50}$  for calcium binding, CuSeCat EE showed improved affinity for trivalent metals (ranging from 1.7-fold to 2.2-fold, with the notable exception of  $\text{Tb}^{3+}$ ). Generally the affinity of CuSeCat EE for trivalent metal ions is inversely proportional to the metal ion size determined for the seven-coordinate state [29]. Figure 4 presents the dependence of the Kemp elimination activity in response to

**Table 2** Kemp elimination activity of the designed mutants in the presence of various metals

Protein	Metal	$(k_{\text{cat}}/K_M)_{\text{max}}$ ( $\text{s}^{-1} \text{M}^{-1}$ )	$M_{50}$ ( $\mu\text{M}$ )	$h$
CuSeCat EE	$\text{Ca}^{2+}$	$29.4 \pm 0.6$	$147 \pm 9$	$2.0 \pm 0.2$
	$\text{Yb}^{3+}$	$14.3 \pm 0.4$	$3.4 \pm 0.2$	$2.7 \pm 0.4$
	$\text{Pr}^{3+}$	$20.0 \pm 1.0$	$4.4 \pm 0.5$	$2.5 \pm 0.6$
	$\text{Nd}^{3+}$	$14.2 \pm 0.5$	$3.5 \pm 0.3$	$2.6 \pm 0.5$
	$\text{Sm}^{3+}$	$9.6 \pm 0.4$	$3.4 \pm 0.3$	$2.8 \pm 0.6$
	$\text{Tb}^{3+}$	$10.1 \pm 0.4$	$3.7 \pm 0.3$	$2.9 \pm 0.7$
	$\text{Yb}^{3+}$	$18.5 \pm 0.2$	$3.2 \pm 0.1$	$2.4 \pm 0.1$
CuSeCat	$\text{Ca}^{2+}$	$42.5 \pm 1.2$	$5.8 \pm 0.5$	$1.6 \pm 0.2$
	$\text{Yb}^{3+}$	$45.7 \pm 1.1$	$6.4 \pm 0.2$	$4.8 \pm 0.6$
	$\text{Pr}^{3+}$	$25.1 \pm 1.6$	$9.6 \pm 0.8$	Fixed at 5
	$\text{Nd}^{3+}$	$23.3 \pm 1.6$	$5.9 \pm 0.7$	$4.4 \pm 1.4$
	$\text{Sm}^{3+}$	$25.7 \pm 1.7$	$5.7 \pm 0.7$	$5.3 \pm 1.7$
	$\text{Tb}^{3+}$	$30.8 \pm 2.0$	$2.7 \pm 0.4$	$5.9 \pm 2.5$
	$\text{Yb}^{3+}$	$65.4 \pm 1.8$	$6.4 \pm 0.3$	$3.8 \pm 0.5$
CuSeCat DD	$\text{Ca}^{2+}$	$45.0 \pm 1.3$	$6.1 \pm 0.6$	$1.0 \pm 0.1$
	$\text{Tb}^{3+}$	$45.9 \pm 5.1$	$3.1 \pm 0.7$	$2.0 \pm 1.0$
CuSeCat D131N	$\text{Ca}^{2+}$	$46.7 \pm 0.6$	$48.4 \pm 0.3$	$1.6 \pm 0.1$
CuSeCat D133N	$\text{Ca}^{2+}$	$41.3 \pm 0.4$	$152 \pm 3$	$1.9 \pm 0.1$

added metal ( $\text{Ca}^{2+}$  and  $\text{Yb}^{3+}$ ). At a metal concentration of less than 10–15  $\mu\text{M}$ , CuSeCat EE can successfully detect  $\text{Yb}^{3+}$  in the presence of comparable concentrations of  $\text{Ca}^{2+}$ . Considering that  $(k_{\text{cat}}/K_M)_{\text{max}}$  for  $\text{Yb}^{3+}$  is higher than that for  $\text{Ca}^{2+}$ , the effective range of the concentration for metal determination is even wider. The other trivalent ions exhibit similar behavior. The overall change of the relative selectivity for the trivalent metal ions over calcium in the study ranges from approximately 30-fold for terbium to approximately 90-fold for praseodymium. CuSeCat DD showed only minor improvement in the relative selectivity for  $\text{M}^{3+}$ . Interestingly, the Hill coefficients for lanthanide binding to CuSeCat are quite high. This can be explained by the higher affinity of the N-terminal domain of CuSeCat (which is identical to that of calmodulin) for  $\text{Ln}^{3+}$  [30]. Binding of  $\text{Ln}^{3+}$  to the N-terminal domain has no effect on the catalytic C-terminal domain and thus results in a more pronounced sigmoidal shape of the activity profile. Therefore, the higher apparent values of the Hill coefficient are not necessarily indicative of an increase in cooperativity. This hypothesis is further supported by the decrease in the  $h$  values upon introduction of S101 and N137 mutations into CuSeCat. The increase in affinity of the C-terminal domain for  $\text{Ln}^{3+}$  makes the contribution of the N-terminal domain less pronounced.

## Conclusions

De novo protein design proved to be a powerful tool for creating new catalysts for unnatural reactions [31–33]. Computationally designed catalysts could be further improved using powerful directed evolution techniques offering catalytic efficiencies on par with those of natural enzymes [34]. Coupling allosteric metal-binding sites with design offers several additional advantages: it provides the protein with the necessary stability, essential for further

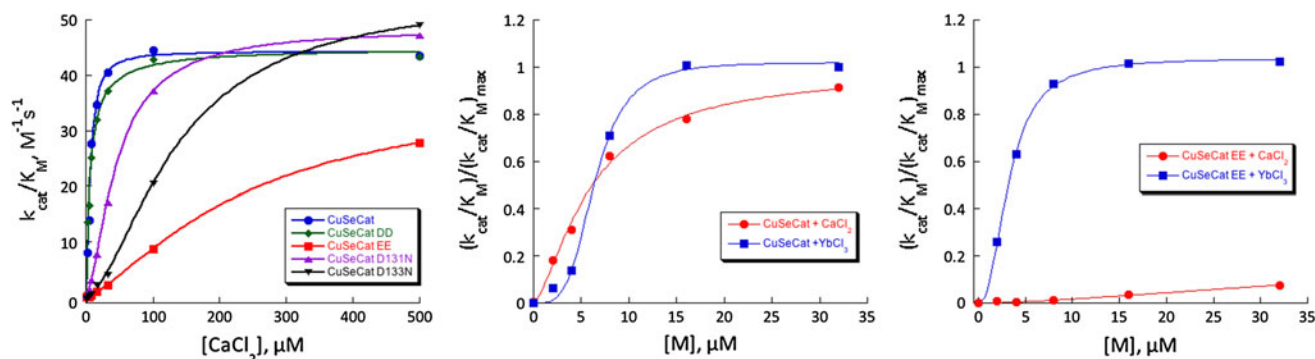


**Fig. 4** Left: Catalytic efficiency of the designed mutants as a function of added  $\text{Ca}^{2+}$ . Middle: Activity of CuSeCat in the presence of  $\text{Ca}^{2+}$  and  $\text{Yb}^{3+}$ . Right: Activity of CuSeCat EE in the presence of  $\text{Ca}^{2+}$  and  $\text{Yb}^{3+}$

improvement; the activity baseline in the absence of the allosteric regulator validates the design, ensuring that the catalyst's function comes from the designed interactions; and finally, it delivers new opportunities for creation of allosterically controlled metal sensors. We showed that the basic principles of metal ion recognition discovered by Falke et al. could be successfully combined with protein design. In this article we demonstrated that the specificity of AlleyCat, a de novo designed catalyst for an unnatural transformation (Kemp elimination) allosterically regulated by  $\text{Ca}^{2+}$ , could be altered to respond to other metals. AlleyCat relies on the energy provided by metal ions binding to EF-hands to catalyze Kemp elimination. By reprogramming the metal-binding domain to bind trivalent metals preferentially to  $\text{Ca}^{2+}$  by a factor of approximately 18-fold to 50-fold (depending on the identity of the trivalent metal), we have established the feasibility of the design of catalytically amplified metal sensors for a variety of metals. The observed selectivity is a result of substantially lower affinity of CuSeCat EE for  $\text{Ca}^{2+}$  and a simultaneous increase in its affinity for trivalent metal ions. The selectivity reprogramming was achieved by a single mutation at position 9 of each of the C-terminal EF-hands producing a catalyst for Kemp elimination, nicknamed CuSeCat EE. The catalytic activity of CuSeCat EE, allosterically regulated by trivalent metal ions, is only mildly affected by the newly introduced mutations. This work established that the metal-binding domain and the catalytic domain are effectively separated and provides a foundation for further selectivity improvement and broadening the scope of the repertoire of metals for sensing. As shown by Nitz et al. [35–37] the luminescence as a result of energy transfer from the tryptophan excited state to lanthanides such as terbium and europium can be used for high-throughput screening for lanthanide binding. Directed evolution methods that are based solely on the Kemp elimination activity can be used to improve sensitivity and selectivity for metals that do not possess distinct photo-physical properties. A concerted effort in the design of switchable enzymes has many environmental, sensing, and metal ion tracking applications.

**Acknowledgments** The authors thank Syracuse University for providing funds for this study, the Beckman Foundation for a scholarship for K.L.M., and Robert P. Doyle for use of his CD instrument.

## References

- Domaille DW, Que EL, Chang CJ (2008) *Nat Chem Biol* 4:168–175
- Luque de Castro MD, Herrera MC (2003) *Biosens Bioelectron* 18:279–294
- Doi N, Yanagawa H (1999) *FEBS Lett* 453:305–307
- Dwyer MA, Hellinga HW (2004) *Curr Opin Chem Biol* 14:495–504
- Miyawaki A, Llopis J, Heim R, McCaffery JM, Adams JA, Ikura M, Tsien RY (1997) *Nature* 388:882–887
- Zhu L, Anslyn E (2006) *Angew Chem Int Ed* 45:1190–1196
- Ostermeier M (2009) *Curr Opin Struct Biol* 19:442–448
- Yoon HJ, Kuwabara J, Kim J-H, Mirkin CA (2010) *Science* 330:66–69
- Korendovych IV, Kulp DW, Wu Y, Cheng H, Roder H, DeGrado WF (2011) *Proc Natl Acad Sci USA* 108:6823–6827
- Blommel PG, Fox BG (2007) *Protein Expr Purif* 55:53–68
- Studier FW (2005) *Protein Expr Purif* 41:207–234
- Rothlisberger D, Khersonsky O, Wollacott AM, Jiang L, DeChancie J, Betker J, Gallaher JL, Althoff EA, Zanghellini A, Dym O, Albeck S, Houk KN, Tawfik DS, Baker D (2008) *Nature* 453:190–195
- Urbauer JL, Short JH, Dow LK, Wand AJ (1995) *Biochemistry* 34:8099–8109
- Radvoyevitch T (2009) *Biol Direct* 4:49
- Masino L, Martin SR, Bayley PM (2000) *Protein Sci* 9:1519–1529
- Marley J, Lu M, Bracken C (2001) *J Biomol NMR* 20:71–75
- Klee CB, Crouch TH, Richman PG (1980) *Ann Rev Biochem* 49:489–515
- Bertini I, Gelis I, Katsaros N, Luchinat C, Provenzani A (2003) *Biochemistry* 42:8011–8021
- Le Clainche L, Plancque G, Amekraz B, Moulin C, Pradines-Lecomte C, Peltier G, Vita C (2003) *J Biol Inorg Chem* 8:334–340
- am Ende CW, Meng HY, Ye M, Pandey AK, Zondlo NJ (2010) *ChemBioChem* 11:1738–1747
- Zondlo SC, Gao F, Zondlo NJ (2010) *J Am Chem Soc* 132:5619–5621
- Moroz OV, Moroz YS, Mack KL, Wu Y, Olsen AB, Cheng H, McLaughlin JM, Raymond EA, Roder H, Korendovych IV (in preparation)
- Drake SK, Falke JJ (1996) *Biochemistry* 35:1753–1760
- Drake SK, Lee KL, Falke JJ (1996) *Biochemistry* 35:6697–6705
- Falke JJ, Drake SK, Hazard AL, Peersen OB (1994) *Q Rev Biophys* 27:219–290
- Ye YM, Lee H-W, Yang W, Shealy S, Yang JJ (2005) *J Am Chem Soc* 127:3743–3750
- Chou JJ, Li S, Klee CB, Bax A (2001) *Nat Struct Biol* 8:990–997
- O'Neil KT, DeGrado WF (1990) *Trends Biochem Sci* 15:59–64
- Snyder EE, Buoscio BW, Falke JJ (1990) *Biochemistry* 29:3937–3943
- Mulqueen P, Tingey JM, Horrocks WD Jr (1985) *Biochemistry* 24:6639–6645
- Samish I, MacDermaid CM, Perez-Aguilar JS, Saven JG (2011) *Annu Rev Phys Chem* 62:129–149
- DeGrado WF, Summa CM, Pavone V, Nastro F, Lombardi A (1999) *Annu Rev Biochem* 68:779–819
- Das R, Baker D (2008) *Annu Rev Biochem* 77:363–382
- Brustad EM, Arnold FH (2011) *Curr Opin Chem Biol* 15:201–210
- Nitz M, Franz KJ, Maglathlin RL, Imperiali B (2003) *ChemBioChem* 4:272–276
- Franz KJ, Nitz M, Imperiali B (2003) *ChemBioChem* 4:265–271
- Nitz M, Sherawat M, Franz KJ, Peisach E, Allen KN, Imperiali B (2004) *Angew Chem Int Ed* 43:3682–3685